TECHNICAL TRANSACTIONS | CZASOPISMO TECHNICZNE
CIVIL ENGINEERING | BUDOWNICTWO

2-B/2016

**DOI: 10.4467/2353737XCT.16.167.5778**

MAREK PIEKARCZYK, JOANNA NYTKO, DAMIAN GIDLEWSKI*

# A STUDY ON THE IMPERFECTION SENSITIVITY OF THE SHELL OF A CYLINDRICAL STEEL TANK

# STUDIUM WRAŻLIWOŚCI IMPERFEKCYJNEJ PŁASZCZA STALOWEGO ZBIORNIKA WALCOWEGO

A b s t r a c t

This paper summarises a study on the imperfection sensitivity of the shell of a steel cylindrical tank. The loadings – normal to the peripheral of the shell and along it were taken into consideration. A bifurcation analysis and then a non-linear analysis with geometric imperfections, which amounted to 2, 5, 10 mm, were conducted. Comparison of the results is given in the form of charts and tables, some conclusions are then drawn.

*Keywords: tank, shell, non-linear analysis, geometric imperfections*

S t r e s z c z e n i e

W artykule przedstawiono ocenę wrażliwości imperfekcyjnej płaszcza stalowego zbiornika walcowego pod obciążeniem prostopadłym do pobocznicy oraz wzdłuż pobocznicy powłoki. Dla zbiornika przeprowadzono liniową analizę bifurkacyjną, a następnie analizę nieliniową z przyjętymi imperfekcjami geometrycznymi, które wyniosły 2, 5, 10 mm. Porównanie wyników obliczeń przedstawiono w postaci wykresów i tabel, a następnie wyciągnięto wnioski.

*Słowa kluczowe: zbiornik, powłoka, analiza nieliniowa, imperfekcje geometryczne*

* Prof. D.Sc. Eng. Marek Piekarczyk, M.Sc. Eng. Joanna Nytko, M.Sc. Eng. Damian Gidlewski, Institute of Building Materials and Structures, Civil Engineering Faculty, Cracow University of Technology.

## 1. Introduction

The designing of steel tanks and other special shell structures, such as silos or chimneys, based on the set of European codes [1–3] in many cases requires the application of sophisticated techniques for computing the behaviour of a construction under load, e.g. FEM. This results directly from the above codes, in particular for structures which are included into higher reliability classes in these codes [4, 5].

The type of analysis which is to be used in the case (Table 1), is given in the standard [6] (Table 2) with respect to a shell theory, a material law and the geometry of a shell ( perfect or imperfect).

Table 1

**Types of non-linear analysis of shell structures**

| Type of analysis | Shell theory | Material law | Shell geometry |
|---|---|---|---|
| Geometrically non-linear elastic analysis (GNA) | non-linear | linear | perfect |
| Materially non-linear analysis (MNA) | linear | non-linear | perfect |
| Geometrically and materially non-linear analysis (GMNA) | non-linear | non-linear | perfect |
| Geometrically non-linear elastic analysis with imperfections (GNIA) | non-linear | linear | imperfect |
| Geometrically and materially non-linear analysis with imperfections (GMNIA) | non-linear | non-linear | imperfect |

With respect to over-ground tanks with cylindrical shells, the methods of numerical analysis indicated in Table 1 apply to the objects classified in the consequence class CC3 according to reliability differentiation [1]. This refers to tanks for toxic liquids, explosive or harmful to the aquatic environment in urban areas, among other uses. For other types of tanks (classes CC1 and CC2) there is the option to use numerical methods, for example, FEM. Imperfections in tanks of consequence classes CC2 and CC3 cannot exceed the fabrication tolerances given in [6, 7].

Cylindrical shells are highly sensitive to imperfection [8]; therefore, significant values of the imperfections can cause a visible change in the local state of stress in the shell of a tank resulting in the failure of the structure [9]. These shells must be checked for buckling limit state (LS3). The GMNIA method of analysis gives the best estimate of the load-bearing capacity in LS3 [10].

Below, a study on the dependence of the carrying capacity of the shell of a sample cylindrical tank with a steel roof on the acquired imperfections was conducted. A potential field of imperfections in the form of waves after buckling was assumed. The amplitudes of the waves were equal to the thickness of the shell multiplied by various total numbers. The maximum fabrication tolerances were taken into account. This is a well-known method of analysis of the carrying capacity of cylindrical shells [11, 12].

## 2. Technical data of the tank

A single-shell steel tank with a domed fixed roof without a catch basin with a capacity of 10,000 m$^3$ for diesel is taken into consideration.

The tank lies in the second zone of snow load and in the first zone of wind load. The shell is made of steel with a grade of S355. The consequence class of the tank is CC3. The basic dimensions of the tank are shown in Fig. 1.

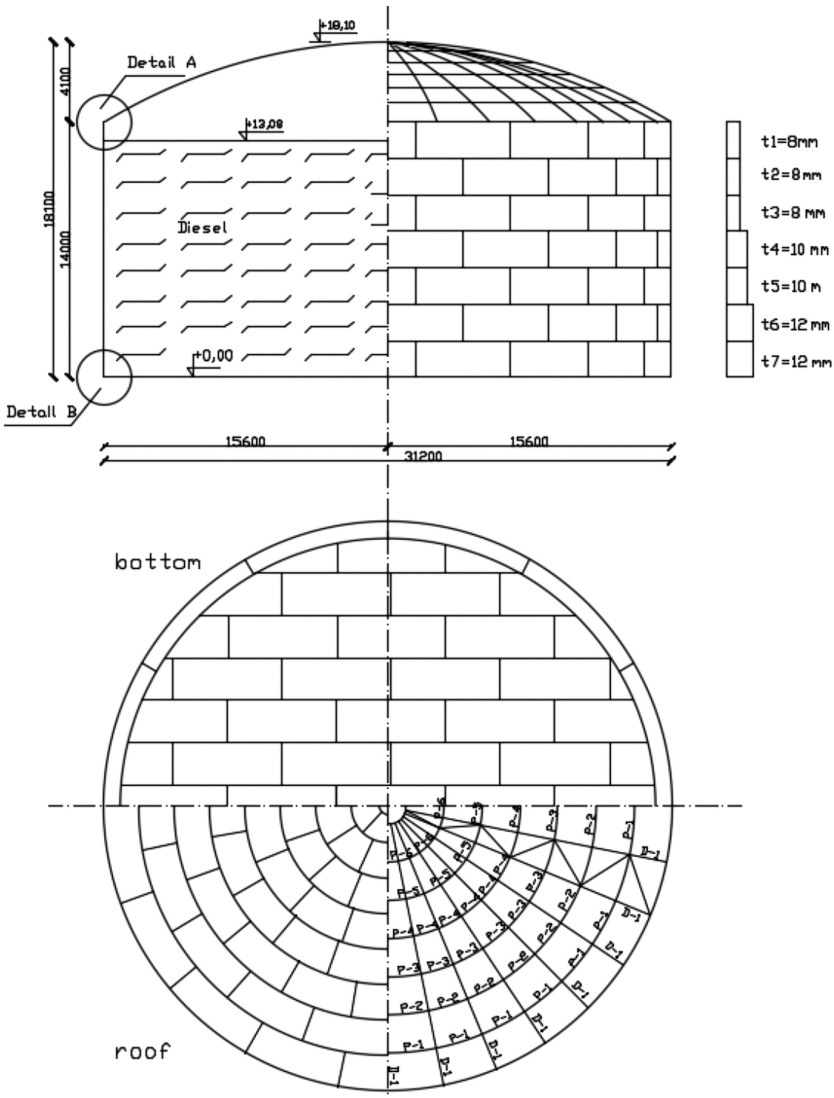


Fig. 1. Geometry of the tank

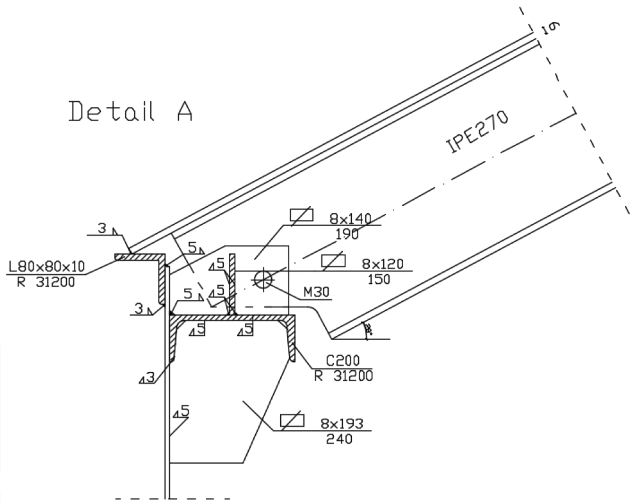


Fig. 1a) Detail A: upper ring

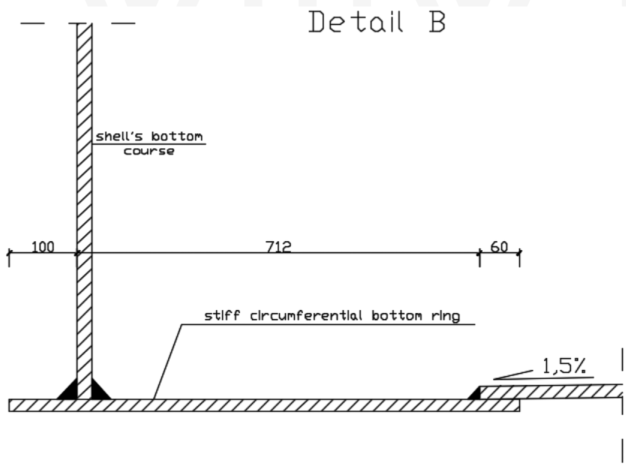


Fig. 1b) Detail B: fixed connection shell bottom

## 3. Parameters of the numerical model in non-linear analysis

The simplified numerical model of a cylindrical shell with a diameter of 31.2 m, depth of 14 m and thickness varying from 8 to 12 mm (Fig. 1) built in Abaqus CAE [13, 14] was divided into 5,488 square (0.5×0.5 m) finite shell elements called S4.

A geometrically non-linear and perfect elastic-plastic material model without hardening was assumed for the Newton-Raphson incremental-iterative method of analysis using a control of loads at first and then a control of displacements. Material parameters are

$f_y$ = 355 MPa, $E$ = 210 GPa, $v$ = 0.3. Stiffening through the use of a ring around the upper edge of the shell around the perimeter (detail A, Fig. 1a) and a full fixing of its other edge in conjunction with the bottom of the tank (detail B, Fig. 1b) were taken into account. The upper ring was substituted in the numerical modelling by a rod element with a very high level of stiffness.

## 4. Shell loaded by pressure normal to the shell surface

The loading shown in Fig. 2 normal to the mantle surface, corresponding with the load situations called suction for pressure below atmospheric and/or an evenly distributed equivalent wind load [1] creates the greatest threat for a cylindrical shell due to the local buckling phenomenon.

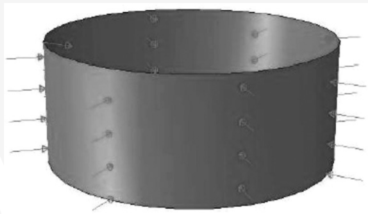

Fig. 2. Pressure normal to the shell surface

In order to obtain the initial shape of the bulged shell for a non-linear analysis with geometrical imperfections GMNIA, a linear bifurcation analysis (LBA) was conducted at the beginning. After a unit loading with a value of 1.0 kPa was applied and magnified, the critical factor $\lambda$ = 2.42 and the buckled form presented in Fig. 3 were achieved.

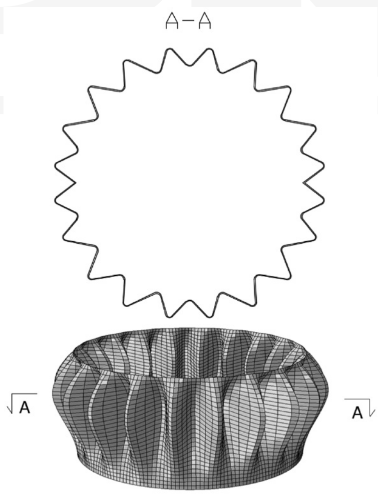


Fig. 3. Buckling of the shell for the normal pressure

A similar bifurcation analysis for the model shown in Fig. 4, built in the Autodesk Robot Structural Analysis 2015 program [15, 16], was performed in order to verify the critical load value obtained in the linear bifurcation analysis in Abaqus.

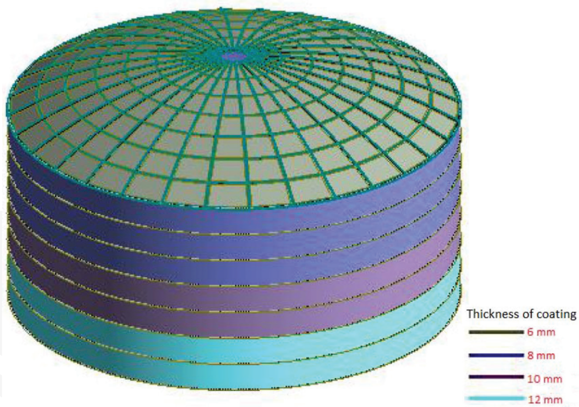


Fig. 4. Model of the tank in Autodesk Robot Structural Analysis 2015. Linear bifurcation analysis

The Robot model includes a dome-shaped roof with IPE 270 girders and a bottom. The bottom rests on the ground of Winkler's type (sand cushion).

For such a calculation model, a critical factor was achieved for the load normal to the shell $\lambda = 2.54$ which is close to the result obtained for the model in the Abaqus.

A non-linear analysis of an ideal (without imperfections) shell model (GMNA) under load was performed thereafter. The value of the limit loading obtained here is similar to the result of the bifurcation analysis for the LBA linear model (Fig. 5) that may validate the non-linear model.

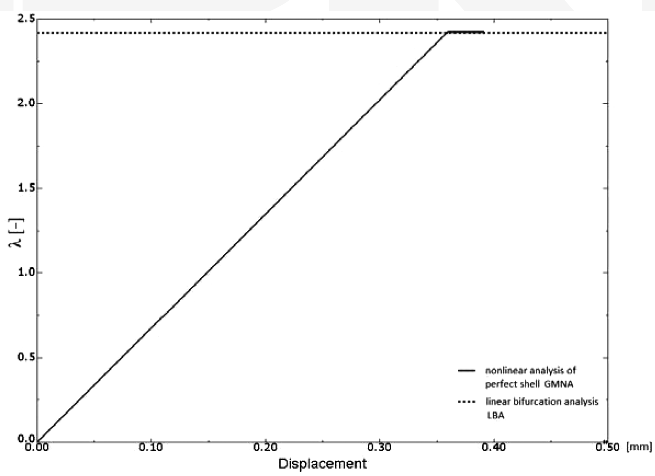


Fig. 5. Path of equilibrium for the analysed shell

The model with the initial imperfection in accordance with the first buckling mode of the linear analysis with a maximum amplitude of waves 2 mm (0.15–0.25 shell thickness) was then subjected to an incremental loading until failure. The deformation of the shell with the map of stress after GMNIA for loading close to the limit value is presented in Fig. 6. A significant decrease of the value of the limit load multiplier λ to about 2.00 was observed (Fig. 7).

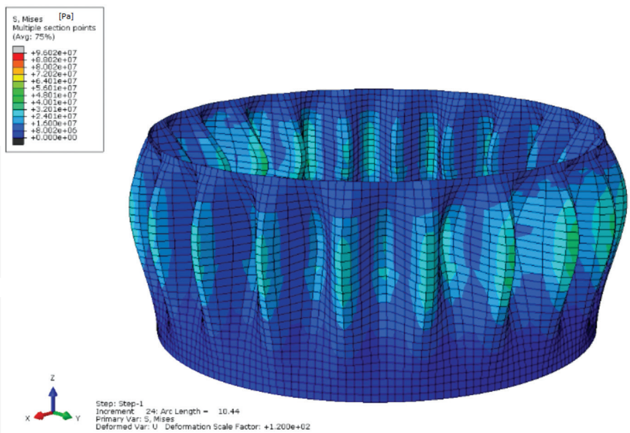


Fig. 6. Deformation of the shell with the map of stress before reaching limit point

Similar analyses were carried out for imperfections: 5 mm (0.42–0.63 shell thickness) and 10 mm (0.83–1.25 mm shell thickness). Ever greater reductions in the carrying capacity of the shell were obtained, respectively, λ = 1.68 and λ = 1.42.

The results of the analyses for the shell with imperfections under a normal load are presented in Fig. 7 and Table 2.

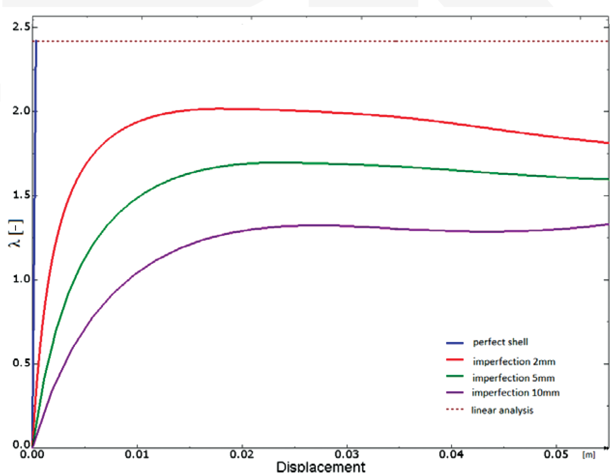


Fig. 7. Result for normal pressure – paths of equilibrium

Table 3

**Decrease in capacity of the shell depending on given imperfection**

| Pressure normal to the shell | | |
|---|---|---|
| Size of imperfection [mm] | Value of limit factor λ | Decrease in capacity [%] |
| 0 | 2.42 | 0.00 |
| 2 | 2.00 | 17.36 |
| 5 | 1.68 | 30.58 |
| 10 | 1.42 | 41.32 |

## 5. Shell subjected to meridional compressive load

Figure 8 shows the shell of the tank under a meridional symmetrical compressive load equally and linearly distributed along the upper edge – this corresponds to the load of the weight of the roof itself, snow on the roof, and suction onto the tank roof resting on the shell.

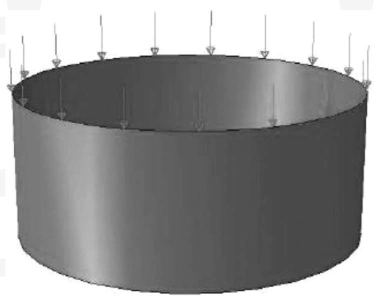

Fig. 8. Scheme of the meridional compressive load on the edge of the shell

Calculations were carried out according to procedures analogous to the case described in Section 4. The critical factor in the bifurcation analysis by means of amplification of a unit load edge 1.0 kN/m was $\lambda = 536$ and a form of the local buckling shown in Fig. 9 was obtained.

An analysis of a non-linear ideal model (GMNA) produced a result for the limit load close to that obtained in the LBA analysis (Fig. 10).

Next, analyses of the model with 2 mm, 5 mm and 10 mm imperfections and the shape obtained previously in LBA, were performed. The results of these analyses are shown in Fig. 10 and in Table 3.

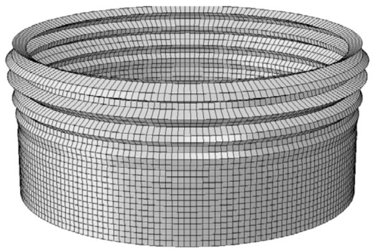

Fig. 9. Buckling form obtained in the linear analysis in program Abaqus for meridional compression

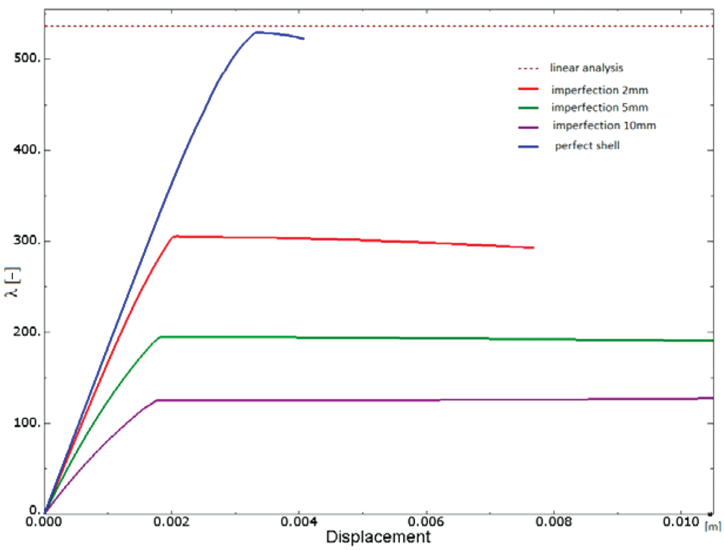


Fig. 10. Results for compressive load – paths of equilibrium

Table 4

**Decrease in capacity for the shell depending upon given imperfection**

| **Compressive loading** | | |
|---|---|---|
| Size of imperfection [mm] | Value of limit factor λ | Decrease in capacity [%] |
| 0 | 536 | 0.00 |
| 2 | 312 | 41.79 |
| 5 | 200 | 62.69 |
| 10 | 136 | 74.63 |

In the first step of loading, an increase of the displacements harmonically contracting along the axis of the periphery of the shell in accordance with the assumed post-bifurcation form of the bulge was found in all the cases (Fig. 11). In the second phase, additional bulges (waves) in a direction perpendicular to the circumference of the cross-section of the shell appeared as shown in Fig. 12.

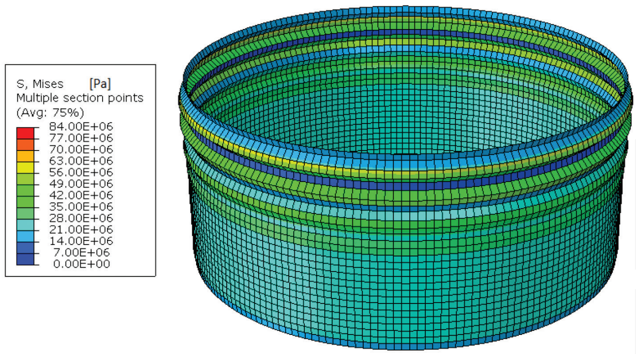


Fig. 11. Deformation of the shell with the map of stress, folds appeared in the meridional direction

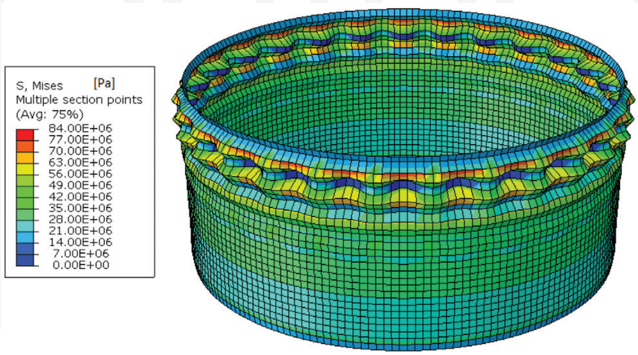


Fig. 12. Deformation of the shell with the map of stress, additional peripheral folds appeared

## 6. Conclusions

The above presented study aimed to investigate the influence of imperfections of certain modes and amplitudes on the load-bearing capacity of the shell of the chosen steel tank. The study suggests the following conclusions:

– the received equilibrium paths (loading vs. displacements) shown in Fig. 7 for the loading perpendicular to the peripheral and in Fig. 10 for the loading along the latter enable the determination of the capacity of the shell in the elastic-plastic range. These paths are analogous to those indicated in figure 8.6 (point 8.7) of the European standard [6] and incorporated here in Fig. 13;

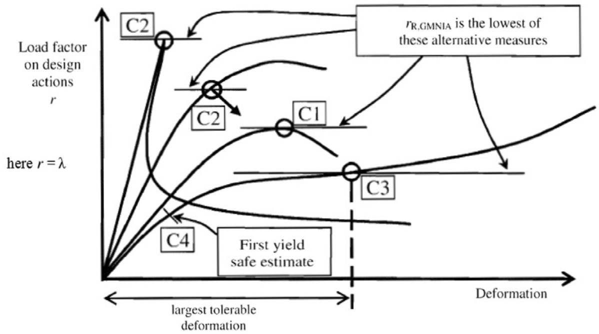


Fig. 13. Definition of buckling resistance from global GMNIA analysis [6]

– the influence of imperfections on the load-bearing capacity of the tank shell is visible in all the cases. For loading normal to the shell, this amounted to 17–41% of the original capacity of the ideal shell, whereas for the gravity loading, it amounted to 42–75%. The imperfections ranged from 2 to 10 mm, which are 14% to 70% of the horizontal and vertical tolerances for the fabrication quality class B and 25% to 125% for class A respectively, according to [6, 7];
– the presence of large imperfections also causes another form of damage to the shell by the development of deformations in two directions – parallel and perpendicular to the periphery (see Fig. 12). In this context, the effect of the interaction of compressive actions in two directions simultaneously should be further investigated. Operating conditions of this kind may occur in tanks, for example, when there is retention of snow on the roof and in the presence of suction inside the tanks.

## References

[1] EN 1993-4-2: 2009 Eurocode 3. Design of steel structures. Part 4–2: Tanks.
[2] EN 1993-4-1: 2007 Eurocode 3. Design of steel structures. Part 4–1: Silos.
[3] EN 1993-3-2: 2006 Eurocode 3. Design of steel structures. Part 3–2: Chimneys.
[4] ECCS, *Buckling of Steel Shells – European Design Recommendations*, 5th Edition, 2014.
[5] Piekarczyk M., Michałowski T., Kowalczyk D., *Examples of Designing Steel Shell Structures According to Eurocodes*, Technical Transactions 1-B/2015, 75-86.
[6] EN 1993-1-6: 2007 Eurocode 3. Design of steel structures. Strength and stability of shell structures.
[7] EN 1090-2: 2008 Execution of steel structures and aluminium structures – Part 2: Technical requirements for steel structures.

[8] Piekarczyk M., *Taking advantage of post-buckling strength in designing of steel structures*, Monograph No. 299, Politechnika Krakowska, Kraków 2004.

[9] Kowalski D., *Naprężenia w płaszczu zbiornika stalowego z lokalnymi deformacjami (Stresses in Steel Tank Shell with Local Deformations of the Shell)*, Inżynieria i Budownictwo, No. 6/2001, 351–353 (in Polish).

[10] Ziółko J., Mikulski T., Supernak E., *Deformacje płaszcza stalowego pionowego zbiornika walcowego spowodowane podciśnieniem (Deformations of the cylindrical vertical steel tank shell due to underpressure)*, Inżynieria i Budownictwo, No. 2/2016, 62–64 (in Polish).

[11] Wójcik M., N. Kuczyńska, Tejchman J., *Analiza wyboczeniowa MES cylindrycznego silosu z blachy gładkiej zawierającego materiał sypki (Buckling FE analysis of cylindrycal metal silo from plain sheets containing bulk solid)*, Inżynieria i Budownictwo, No. 11/2014, 640–643 (in Polish).

[12] Iwicki P., Tejchman J., Chróścielewski J., *Dynamic FE simulations of buckling process in thin-walled cylindrical metal silos*, Thin-Walled Structures, No. 84, 2014, 344–359.

[13] Program *Abaqus(CAE),* Theory manual, version 6.10., Hibbit, Karlsson&Sorensen Inc.2010.

[14] Witkowski W., Chróścielewski J., Buczyński S., Deszkiewicz K., Sobczyk B., *Wprowadzenie do modelowania MES w programie Abaqus (Introduction to FEM Modelling in Abaqus Program)*, Politechnika Gdańska, Gdańsk 2014, (in Polish).

[15] Program *Autodesk Robot Structural Analysis 2015.*

[16] Gidlewski D., *Projekt stalowego zbiornika na olej napędowy. Nieliniowa analiza wyboczenia powłoki płaszcza zbiornika (Design of Steel Tank for Diesel Oil. Nonlinear Analysis of Shell Buckling)*, Praca dyplomowa magisterska (Diploma work of Master's degree), supervised by prof. M. Piekarczyk, Politechnika Krakowska, Kraków 2015.